



# Alternatives of resorcinol in carbon black filled belt skim compound: A sustainable approach to make tire

Pankaj Kumawat<sup>1</sup> | Jagannath Chanda<sup>1</sup> | Sanjit Kumar Das<sup>1</sup> | Anshu Ghosal<sup>2</sup> | Saikat Das Gupta<sup>1</sup> | Rabindra Mukhopadhyay<sup>1</sup>

<sup>1</sup>Material Research Group, Hari Shankar Singhanian Elastomer and Tyre Research Institute, Mysore, India

<sup>2</sup>Research and Development, Singh Plasticisers and Resins (I) Pvt. Ltd., Rajasthan, India

## Correspondence

Saikat Das Gupta and Jagannath Chanda, Material Research Group, Hari Shankar Singhanian Elastomer and Tyre Research Institute, Mysore 570016, India.

Email: saikat.dasgupta@jkmil.com and jagannath.chanda@gmail.com

## Abstract

As per global trends, new legislation, regulations, and restrictions on the use of hazardous materials with respect to environmental concerns, it has become necessary to eliminate resorcinol from the rubber compound as it was generating carcinogenic fumes during processing at high temperature. In this research, two non-hazardous phenolic resins [A] and [B] were explored, in place of resorcinol, in a typical PCR tire belt skim compound. The entire study includes three phases. In Phase I, resorcinol was substituted with both the resins and it was revealed that they have potential to function as resorcinol in rubber-brass bonding mechanism with few limitations, primarily as low cure rate. In Phase II, it was adjusted by incorporating TBBS as an additional accelerator but an abrupt loss in extent of adhesion retention was noticed for aged samples. It leads to further investigation in Phase II compositions. In Phase III, a little amount of precipitated silica was formulated, which results into a significant revival of adhesion retention. Eventually, both the compounds were showing faster vulcanizing characteristics, improved aged and un-aged properties, higher dynamic stiffness, and lower hysteresis. Compound [B] showed best performance in all the properties except fatigue crack growth rate in low strain percentage.

## KEYWORDS

adhesion, aging and hysteresis, belt skim compound, PCR tire, phenolic resins

## 1 | INTRODUCTION

Traditionally, resorcinol (Benzene-1, 3-diol) is employed as adhesion-promoting system along with hexamethoxy methylmelamine (HMMM) in rubber compound, used to coat brass plated-steel belt and carcass in radial tires.<sup>[1-3]</sup>

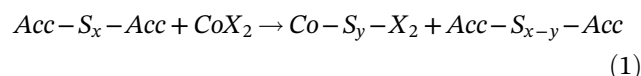
Resorcinol is classified as a hazardous compound as it is a skin irritant, a potential endocrine-disrupting ingredient, and a marine water pollutant. Resorcinol readily sublimes as it attains its melting temperature (108.8°C) and emits carcinogenic fumes and obnoxious odor during

mixing, extrusion, and calendaring processes. In addition, the condensed resorcinol vapors tend to stick to cooler surfaces and form white dendrites. These dendrites absorb atmospheric moisture and become tacky, leading to mold fouling, silo sticking, and causing handling issues.

In the present investigation, resorcinol has been replaced with two differently modified phenolic resins, commercial names-POWERPLAST PP 1872 [A] and POWERPLAST PP 1963 [B]. These resins are non-fuming, non-hygroscopic, highly processable, non-resorcinolic,

and environment friendly. In rubber industries, precondensed resorcinol-formaldehyde resin is commonly employed as a methylene acceptor in place of resorcinol. But it contains enough free-resorcinol to generate fumes on higher compound processing temperature. The hygroscopicity of this material is another concern.<sup>[4]</sup> The rubber compound used for coating the brass-plated steel belt specially contains a high level of elemental sulfur. Major part of this sulfur is utilized in adhesion bonding and rest of part function as a curative. During bonding mechanism, sulfur reacts with copper, coated on steel cords, at vulcanization temperature and forms bonds between rubber and brass. The chemical composition of brass plating and its thickness largely influences the bonding strength. In brass, copper to zinc ratio (65/35) wt% was found to be optimum composition for best adhesion.<sup>[5,6]</sup> As investigated earlier by Van Ooij that copper sulfide ( $\text{Cu}_x\text{S}$ ) grows as dendrites into the uncured viscous rubber for bonding before the vulcanization reaction proceeds.<sup>[7,8]</sup> Beecher<sup>[9]</sup> and Persoone<sup>[10]</sup> also studied the mechanism of brass-rubber bonding and proposed chemical cross linking via the Cu-S-rubber (natural rubber) linkages. Similar studies were also carried out by G. S. Jeon<sup>[3,11]</sup> and concluded that the rubber-brass adhesion is the result of Cu-S-rubber bonds formation. In order to enhance performance and durability of the radials, it becomes essential to improve the adhesion strength via optimum copper sulfide ( $\text{Cu}_x\text{S}$ ) layer formation.<sup>[12]</sup> This layer also known as interlayer, which degrades under hostile environmental and operating conditions of hysteresis, high stress, high strain, and eventually causes adhesion failure. Therefore, this interlayer needs to be protected for durability in terms of adhesion.<sup>[1]</sup> In order to protect the interlayer several materials such as cobalt salts of carboxylic acid,<sup>[7,13]</sup> zinc borate,<sup>[14]</sup> resorcinol, HMMM, and hexamethylenetetramine (HMT) are incorporated as adhesion promoter. Resorcinol is always formulated along with either HMMM or HMT where resorcinol functions as formalin acceptor and HMMM/HMT as formalin donor.<sup>[3]</sup> The use of HMT is restricted due to its toxicity as it liberates ammonia and formaldehyde on thermal decomposition.<sup>[15]</sup> At typical vulcanization temperature, the polar resorcinol molecules migrate to the rubber-metal interface and start to form a highly crosslinked complex structure by reaction with formalin donor. This complex serves to protect the interlayer by restricting the conversion of  $\text{Cu}_2\text{S}$  into  $\text{CuS}$ .<sup>[7,8]</sup> The  $\text{Cu}_2\text{S}$  form of interlayer is flexible and amorphous while  $\text{CuS}$  form is brittle and crystalline, hence breakage of bonding occurs, leading to adhesion failure.<sup>[1]</sup> The combination of resorcinol and HMMM/HMT is known as two component adhesion promoter system.<sup>[2]</sup> Moreover, the cobalt salts such as cobalt stearate, cobalt boroacrylate are

currently being used individually and thus it is known as one component adhesion promoter system.<sup>[13,16]</sup> Above mentioned both system are also used jointly for better adhesion bonding and durability.<sup>[17-18]</sup> It is assumed behind the adhesion improvement and protection by cobalt salts that the accelerator-sulfur complex formed during vulcanization, reacts with it and forms a cobalt complex.<sup>[3]</sup>



where *Acc* is accelerator, *S* is elemental sulfur, *x* and *y* are no. of molecules, and  $\text{CoX}_2$  is cobalt salt. This complex helps in migration of copper to form interlayer with optimum thickness. It is also believed that cobalt salts inhibit the dezincification reaction and enhance the bond strength.<sup>[6]</sup> A significant amount of work on metal to rubber adhesion was also carried out by M. Liu et al.<sup>[19]</sup>

In order to develop optimum bond strength, it is important that the rate at which the resorcinol-HMMM reaction occurs be comparable to that at which vulcanization reaction proceeds.<sup>[3]</sup> The high reactivity of resorcinol allows the two reaction rates to be co-ordinated with each other. Other formalin acceptors like phenolic resins, are not typically successful in this application as they are less reactive than the resorcinol, therefore, the experimental resins have been developed with proprietary modifications to enhance their reactivity as high as resorcinol.

PP-1872 [A] is a functional phenolic resin. In addition to the hydroxyl groups of phenol, other proprietary functional groups have been added. These functional groups increase the reactivity of the resin-HMMM reaction that takes place simultaneously as the vulcanization of rubber compound proceeds. Chemically this material is resorcinol free.

PP-1963 [B] is a phenolic resorcinol-formaldehyde resin, where the free (unreacted) resorcinol is reduced to less than 0.1%, thereby eliminating exposure to unreacted resorcinol completely. This resin is a copolymer of resorcinol, phenol, and alkyl substituted phenol. The copolymerization of resorcinol with phenols and substituted phenols changes the characteristics of the resulting resin molecules and hence its reactivity with HMMM. The properties of the resultant crosslinked structure are also likely to change with the ratio of the different copolymers.

In the era of sustainable technology, several researchers extend their support to invent new material for the replacement of carcinogenic and hazardous substance with respect to environmental safety. This study aims to replace resorcinol by 1:1 ratio with two non-hazardous phenolic resins called resin [A] and [B] to develop advanced belt skim compound without

affecting rheometric, physical, and adhesion properties. It was conducted in three phases. Fatigue crack growth (FCG) rate has also been studied for the above compounds by using Tear and Fatigue Analyzer (TFA) at 70°C with different strain percentages. Details of experimental procedure and result analysis are consolidated in further sections.

## 2 | EXPERIMENTAL DETAILS

### 2.1 | Raw materials

All the materials used in this investigation are tabulated in Table 1.

The experimentally modified phenolic resins [A] and [B] were procured from Singh Plasticizers and Resins (I) Pvt. Ltd., India. Both resins are bead shaped light red-dish colored solid and odorless.

#### 2.1.1 | Chemical characterization of experimental resins

##### *Chemical analysis*

The chemical analysis of resins was carried out and the test results obtained are depicted in Table 2. The free resorcinol content in resin [B] was found < 0.1% as claimed by manufacturer.

##### *TGA analysis*

The thermogravimetric analysis of resorcinol and resin [A] and [B] was performed in accordance with ISO 11358 by Pyris 1 TGA (Perkin Elmer, USA) to determine the thermal stability and volatility of the materials. The weight loss data versus temperature are given in Table S1.

The non-fuming nature of both the resins can be explained on the basis of their TGA analysis (Figure 1 and Table S1). The resorcinol degraded completely before reaching 250°C whereas the experimental resins show a weight loss of less than 4% at the same temperature. The degradation peaks obtained through derivative of thermogravimetry (DTG) plots for resorcinol, [A] and [B] are 206, 648, and 643°C, respectively.

### 2.2 | Preparation of rubber compounds

#### 2.2.1 | Formulation(s)

The compositions used in this entire study are given in Table 3 along with mixing sequence. The ratio of

**TABLE 1** Raw materials used in this investigation

Ingredients	Trade name	Manufacturer
Natural rubber	RSS #4	J.K.Industries Ltd., Cochin, India
Carbon black	N326	Hi-Tech Carbon, Renukoot, India
Peptizer <sup>a</sup>	Peptizol 11	Acmechem Ltd., Ankleshwar, India
Zinc oxide	White seal	Himalaya Oxide Pvt. Ltd., Mysore, India
Process oil	PANOIL 2800	Raj Petro Pvt. Ltd., Chennai, India
Precipitated silica <sup>b</sup>	Ultrasil VN3 GR	Degussa Insilico, Ltd., India
Insoluble sulfur <sup>c</sup>	Crystex HD OT20	Eastman Chemicals, Malaysia
Cobalt salt <sup>d</sup>	Manobond 680C	OMG Asia Pacific Ltd., Manchester, UK
Resorcinol	—	Atul Ltd., Gujarat, India
Stearic acid	—	Godrej Ind. Ltd., India
6 PPD <sup>e</sup>	Vulkanox 4020	Lanxess India Pvt. Ltd., Bharuch, India
DCBS <sup>f</sup>	Mercure DCBS	NOCIL, Mumbai, India
TBBS <sup>g</sup>	Pilcure MOR	NOCIL, Mumbai, India
TMQ <sup>h</sup>	Pilnox TDQ	NOCIL, Mumbai, India
HMMM 65 <sup>i</sup>	Cyrez 964	Allnex, USA
CTP <sup>j</sup>	Pilgard PVI	NOCIL, Mumbai, India
Brass-plated steel cord <sup>k</sup>	S345	Bekaert Industries Pvt. Ltd., Pune, India

<sup>a</sup>2, 2'-Dibenzamidodiphenylsulfide (40 wt%) active content in clay carrier.

<sup>b</sup>Silicon dioxide (SiO<sub>2</sub>).

<sup>c</sup>Insoluble sulfur treated with (20 wt%) naphthenic oil.

<sup>d</sup>Cobaltborylate (Cobalt content, 23 wt%).

<sup>e</sup>N-phenyl-N'-(1,3-dimethylbutyl) p-phenylene-diamine.

<sup>f</sup>N,N' Dicyclohexyl-2-benzothiazolsulfenamide.

<sup>g</sup>N-tert-Butyl-2-benzothiazolsulfenamide.

<sup>h</sup>1,2-dihydro-2,2,4-trimethyl-quinoline.

<sup>i</sup>Hexamethoxymethyl melamine (65 wt%) active content in silica carrier.

<sup>j</sup>N-Cyclohexylthiophthalimide.

<sup>k</sup>Steel cord (3×0.30 HT).

resorcinol/resins with the HMMM was kept 1:1 in entire study.

The resorcinol and experimental resins were incorporated in master II compound, above their softening point to ensure complete melting and uniform dispersion. While HMMM was added in final batch along with curatives at lower dump temperature primarily because of its high reactivity with resorcinol.

Sl. No.	Test parameter	Test method	Test results	
			Resin [A]	Resin [B]
1	Softening point (°C)	ISO 28641	106.0	104.0
2	Ash content at 850°C for 1 h (%)	ISO 28641	0.08	0.06
3	Heat loss at 105°C for 2 h (%)	ISO 28641	0.13	0.17
4	Moisture by KF titrator (%)	ISO 15512	0.19	0.12
5	Free phenol (%)	ISO 119	0.41	0.22
6	Free resorcinol (%)	HPLC	0.00	0.04

**TABLE 2** Chemical analysis of Resins [A] and [B]

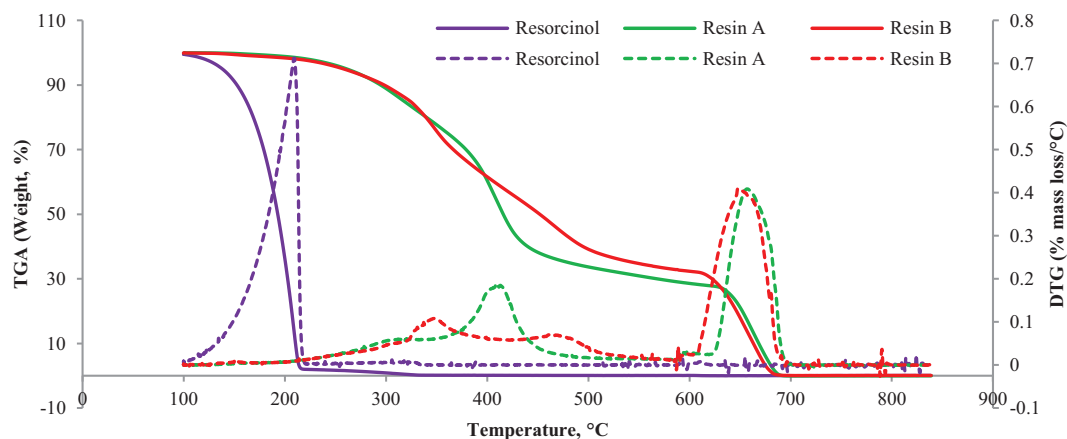


**FIGURE 1** Thermogravimetric analysis of resorcinol, resins [A] and [B]. TGA (solid line) and DTGA (dashed line) [Color figure can be viewed at [wileyonlinelibrary.com](http://wileyonlinelibrary.com)]

### 2.2.2 | Mixing procedure

All the batches were mixed in accordance to ISO 2393 using a 1.6 L capacity laboratory internal mixer (Stewart Bolling, Hudson, OH, USA). Mixing procedures followed for master-I, II, and final batches are given in Table S2. In all phases, control compound was mixed and tested repeatedly along with the experimental compounds to minimize the variations.

### 2.3 | Sample preparation and aging

All the testing specimens were molded using compression molding technique in electrically heated hydraulic curing press (Hind hydraulics and engineers, India) at 150 kg/cm<sup>2</sup> pressure in accordance to ISO 2393. The test specimens for adhesion, physical, and resilience were cured at 160°C for thrice  $t_{c90}$ , 160°C for twice  $t_{c90}$ , and 141°C for 60 min, respectively.

The tensile test specimens were given two type of accelerated aging: (i) Aerobic thermal aging: as per ISO 188 at 70°C for 7 days; (ii) Anaerobic thermal aging: tensile slab molding continued at 130°C for 16 h after giving

normal curing time. The adhesion samples were given four kinds of aging treatments: (i) Heat aging: in oven (Prolific engineers, India) at 100°C for 2 days; (ii) Salt aging: rubber part of cured pads immersed into 10% aqueous solution of NaCl for 7 days, (iii) Humid aging: in humidity chamber (Kasco Industries, Pune, India) at 95% relative humidity, 93.3°C for 14 days, and (iv) Overcuring: molding at 160°C for giving twice time of normal curing time.

### 2.4 | Physical testing and characterization

#### 2.4.1 | Curing characteristics

The curing characteristics were determined using MDR2000E (Alpha Technology, Bellingham, USA) as per ISO 6502 at 160°C for 30 min. Cure rate index (CRI), which is measure of cure reaction rate, can be calculated using the following equation:

$$CRI = \frac{100}{t_{c90} - t_{s2}} \quad (2)$$

**TABLE 3** Formulations (Phases I, II, and III)

Ingredients, phr <sup>a</sup>	Phase I			Phase II		Phase III	
	Control	Resin [A]	Resin [B]	Resin [A]	Resin [B]	Resin [A]	Resin [B]
Master I							
RSS #4 (NR)	100	100	100	100	100	100	100
N326 Carbon black	60	60	60	60	60	60	60
Process oil	6	6	6	3	3	5	5
Master II							
Cobalt boracylate	1	1	1	1	1	1	1
Resorcinol	2.1	0	0	0	0	0	0
Resin [A]	0	2.1	0	2.1	0	2.1	0
Resin [B]	0	0	2.1	0	2.1	0	2.1
Ppt. Silica	0	0	0	0	0	5	5
Final							
Insoluble sulfur	7	7	7	7	7	7	7
HMMM	3.2	3.2	3.2	3.2	3.2	3.2	3.2
DCBS	0.7	0.7	0.7	0.7	0.7	0.7	0.7
TBBS	0	0	0	0.7	0.7	0.7	0.7
CTP	0.2	0.2	0.2	0.15	0.15	0.15	0.15

Note: Other ingredients used are DBD, ZnO, stearic acid, 6 PPD, TMQ with dose 0.2, 5.0, 3.0, 2.2, 2.2 phr, respectively.

<sup>a</sup>Phr, parts per hundred rubber.

where,  $t_{c90}$  (min) is the optimum cure time and  $t_{s2}$  (min) is the scorch safety time.

#### 2.4.2 | Mooney viscosity and Mooney scorch

The Mooney viscosity and Mooney scorch (MS) tests were performed by using MV2000E (Alpha technology, Bellingham, USA) in accordance to ISO 289.

#### 2.4.3 | Stress-strain properties

UTM Zwick Z010 from Zwick, Germany was used in determining the stress-strain properties in accordance to ISO 37. The retention and change in physical properties after aging (A) are calculated by using Equations (3) and (4), respectively.

$$\text{Retention, \%} = \frac{\text{Aged value}}{\text{Unaged value}} \times 100 \quad (3)$$

$$A (\pm), \% = (\text{Retention, \%}) - 100 \quad (4)$$

Here (–) sign indicates a drop and (+) sign indicates a rise in property. After aging tensile strength (TS) and

elongation at break (EB) tend to drop while modulus tends to rise.

#### 2.4.4 | Hardness

MUHT from Gibitre Instruments, SRL, USA was used to measure the Shore A type hardness following ISO 7619.

#### 2.4.5 | Rebound resilience

Schob pendulum type rebound resilience tester (Zwick, Germany) was used to determine resilience by following ISO 4662 method.

#### 2.4.6 | Cross link density

The cross link density (CLD) for all the rubber vulcanizates was determined by the equilibrium solvent swelling method and calculated using Flory-Rehner equation (Equation 5).<sup>[20]</sup>

$$X = - \frac{\ln(1 - Vr) + Vr + (Vr)^2}{2 \times \rho_r \times Vs \times (Vr)^{1/3}} \quad (5)$$

where  $X$  is the CLD ( $\text{mol}/\text{cm}^{-3}$ ), ( $V_r$ ) is the volume fraction of the swollen gel, ( $\chi$ ) is the rubber-solvent interaction parameter, ( $\rho_r$ ) is the density of the raw rubber, and ( $V_s$ ) is the molar volume of the solvent.

### 2.4.7 | T-pull adhesion

The Adhesion tests were performed on UTM Zwick 1445 (Zwick, Germany) as per ASTM D2229 and results reported in the form of pull out force. The compound coverage was captured by optical microscope (Leica Wild M10 from Germany). Percentage adhesion retention after aging was calculated by Equation (3).

### 2.4.8 | Dynamic mechanical analysis

These analysis were performed on DMA VA4000 (Metravib, France) in tension-compression mode as per ISO 4664 following test configuration: frequency; 10 Hz, strain; 1% and temperature; 30, 70, and 100°C.

### 2.4.9 | FCG measurement

TFA (Coefeld, Germany) was used for FCG measurements in pure shear mode.<sup>[21-23]</sup> Table 4 shows the test conditions.

The crack growth rate ( $\text{mm}/\text{cycle}$ ) is calculated with the help of the following equation:

$$\text{FCG rate} = \frac{dc}{dn} \quad (6)$$

where  $c$  is the crack length and  $n$  is the number of cycles.

Tearing energy is calculated by the following equation:

$$T = Wl_0, \quad (7)$$

where  $T$  is the tearing energy ( $\text{N}/\text{mm}$ ),  $W$  is the elastic strain energy, and  $l_0$  is the grip to grip separation.

In this test, crack growth rate follows a power law<sup>[24]</sup> given by following equation:

$$\frac{dc}{dn} = BT^\beta \quad (8)$$

where  $B$  and  $\beta$  are the material constants and dependent on the material's nature under testing.

**TABLE 4** Test conditions used in FCG measurement

Test parameters	Values
Test temperature ( $^{\circ}\text{C}$ )	70
Strain (%)	10, 15, 20, 25, 30
Repeating frequency (Hz)	4
Pulse frequency (Hz)	10
Wave form	Gaussian

Abbreviation: FCG, fatigue crack growth.

## 3 | RESULTS AND DISCUSSION

As per the experimentations were carried out, the results and discussion part can also be subdivided into three parts, Phases I, II, and III.

### 3.1 | Phase I

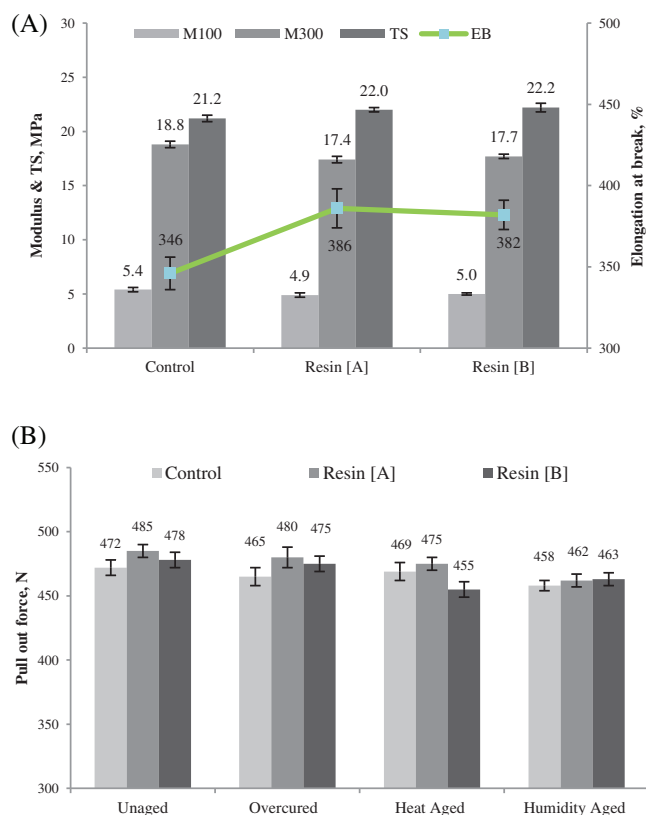
Table 5 illustrates the cure characteristics of the compounds, prepared using formulation shown earlier in Table 3, Phase I. On replacing the resorcinol by resins, both compounds [A] and [B] are showing slower cure behavior, greater values of  $t_{c90}$  ( $\sim 30\%$ ) or lower CRI ( $\sim 22\%$ ), and longer scorch safety time ( $t_{s2}$ ) by  $\sim 49\%$ . The lower values of minimum torque ( $M_L$ ) and maximum torque ( $M_H$ ) over control compound for resin [A] and [B] indicate lower viscosity and lower modulus of the compound, respectively. However, the quit similar torque change ( $\Delta T$ ) values revealed equal extent of CLD<sup>[22]</sup> for all three compounds. This is further complemented by determination of CLD (Figure 4). The Mooney viscosities of the experimental compounds were found  $\sim 6\%$  lower than the control.

The lower  $M_L$ ,  $M_H$ , and viscosity data for resin [A] and [B] are due to the plasticization effect by the resin samples. Similar results were also earlier confirmed by R B Durairaj<sup>[25]</sup> that the phenolic and resorcinolic resins have a potential of plasticization, leading to reduction in compound viscosity and thus provide better processing. The resins are the low molecular weight products, thus easily and uniformly dispersed in the rubber compound matrix, gives lower MV by reducing overall molecular weight of the uncured compound. Both resins are showing quite same effects on physical properties summarized in Figure 2(A). Owing to the plasticization effect by resins, the compound hardness and modulus are decreased, thereby elongation increased. Hardness values noticed for Control, [A] and [B] are 79, 76, 76, respectively. Hardness and modulus at 100% (M100) as well as 300% strain (M300) of the resin [A] and



**TABLE 5** Cure characteristics and Mooney viscosities (Phase I)

Test parameter	Control	Resin [A]	Resin [B]
Minimum torque, $M_L$ (dN.m)	1.63	1.25	1.24
Maximum torque, $M_H$ (dN.m)	31.91	31.23	31.34
$\Delta$ Torque (dN.m)	30.28	29.98	30.10
$t_{S2}$ (min)	1.45	2.12	2.08
$t_{C50}$ (min)	5.68	6.64	6.63
$t_{C90}$ (min)	11.81	15.34	15.32
CRI ( $\text{min}^{-1}$ )	9.7	7.6	7.6
ML(1+4)@100° C (MU)	67	64	63

**FIGURE 2** (A) Physical properties; showing less compound modulus and higher elongation at break (EB) and comparable tensile strength (TS); (B) showing comparable adhesion properties (pull-out force) of un-aged as well as aged samples as compared to control [Color figure can be viewed at wileyonlinelibrary.com]

[B] are decreased by  $\sim 8$ – $10\%$  while EB increased by  $\sim 12\%$ . Tensile strength for all compounds has been found almost similar.

The adhesion data are presented in Figure 2(B) in terms of pull-out forces. As observed from Figure 2(B), the un-aged as well as aged adhesion properties for Resin [A] and [B] are significantly comparable ( $\pm 5\%$  variation) with respect to control. This fact is attributed to the synthesis of protecting interlayer at the interface by reaction

between resin and HMMM at vulcanization temperature.<sup>[12]</sup> These encouraging adhesion properties for resin based compounds, strongly suggested to fine tune the formulation in order to resolve limitations like slower cure and lower viscosity. As this way the belt skim compound can be made free from hazards of resorcinol use.

### 3.2 | Phase II

In Phase II, few modifications have been made in the resin-based compositions. These are: (i) In order to boost cure rate, 0.7 phr of an additional accelerator TBBS, was added and retarder dose reduced from 0.20 to 0.15 phr; (ii) To increase compound viscosity, process oil loading was reduced from 6.0 to 3.0 phr. These changes were made to meet the phase II resin based compound's properties in line with control compound. Due to some other modifications beside resins, these compounds would be known as Compound [A] and Compound [B] instead of Resin [A] and Resin [B]. Table 6 describes the rheometric properties obtained using modified formulation. Since the MV of the compound is dependent on the process oil loading,<sup>[26]</sup> the experimental compounds have been showed higher viscosity than Phase I, on reducing process oil dose and this time it is found almost equal to the control. The other changes obtained in phase II compound's properties are: reduced  $t_{S2}$  (still  $\sim 8\%$  higher), reduced  $t_{C90}$  values (faster cure,  $\sim 15\%$ ), and higher CRI ( $\sim 21\%$ ) as compared to control. This is predominantly due to the decreased retarder and increased accelerator dose. These all test results are desirable for rubber compound under study.

On addition of another accelerator, the sulfur to accelerator (S/Ac) ratio of the phase II compounds was reduced from 8:1 to 4:1. Due to this modification, the compound CLD was increased (Figure 4), which results into an enhancement in modulus. M100 and M300 (Figure 3) were enhanced by  $\sim 11$  and  $\sim 4\%$ , respectively, along with TS. An increase in CLD was observed with

Test parameter	Control	Resin [A]	Resin [B]
Minimum torque, $M_L$ (dN.m)	1.61	1.64	1.66
Maximum torque, $M_H$ (dN.m)	32.18	33.78	34.08
$\Delta$ Torque (dN.m)	30.57	32.14	32.42
$t_{S2}$ (min)	1.39	1.51	1.50
$t_{C50}$ (min)	5.61	4.40	4.38
$t_{C90}$ (min)	11.81	10.10	10.00
CRI ( $\text{min}^{-1}$ )	9.6	11.6	11.8
ML(1+4)@100° C (MU)	68	69	69

**TABLE 6** Cure characteristics, Mooney viscosities, and scorch (Phase II)

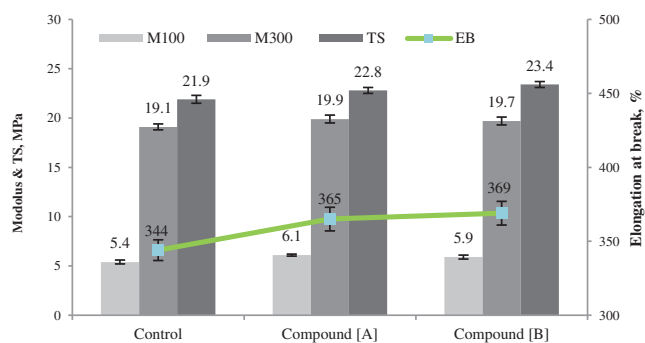


**FIGURE 3** Physical properties; shows desirable higher modulus, tensile strength (TS) and elongation at break (EB) for both compounds [A] and [B] over control [Color figure can be viewed at wileyonlinelibrary.com]

decreasing S/Ac ratio.<sup>[27]</sup> However, the EB for both experimental compounds are found to be greater than control compound, indicates the reinforcing nature of newly made compounds. TS of all the compounds are obtained as similar as observed previously in Phase I.

Hardness values noticed for Control, [A] and [B] are 79, 81, 81, respectively. It has been equally increased by ~6–7% for both compounds, which might be due to increase in CLD (Figure 4).<sup>[20]</sup>

In case of adhesion property, un-aged data have been observed comparable ( $\pm 5\%$  variation) with the control. This could be due to the sufficient bonds (interlayer) formation. On the other hand, an abrupt decline in the extent of adhesion retention noticed as the cured specimens were subjected to different accelerated aging treatments that is heat, humid, salty water, and so forth (Figure 5). Reduction in aged adhesion values are due to the shorter scorch safety time. As earlier studied by Van Ooij,<sup>[1,8]</sup> the delayed action sulfenamide accelerator, DCBS is only being employed in the brass-plated steel skim compound. This provides sufficient scorch safety time for the formation of interlayer as well as synthesis of highly crosslinked network structure or complex at the rubber-metal interface. But in this stage of investigation,

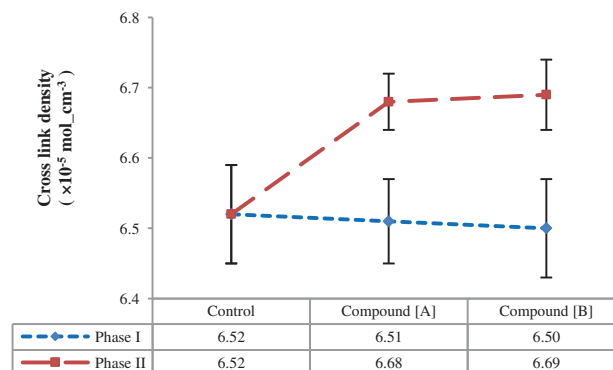


**FIGURE 4** Cross link density (CLD) of Phases I and II compounds. Phase II compounds [A] and [B] have been showed increased CLD [Color figure can be viewed at wileyonlinelibrary.com]

TBBS was also used as booster for faster vulcanization reaction. TBBS provided less scorch safety time for complex formation at the interface. This complex provides protection to the interlayer under hostile environmental conditions and retains adhesion. Therefore, in case of unaged adhesion, comparable values are observed due to the formation of sufficient interlayer as compared to control. But during aging, the interlayer was not protected by the complex as it might not be formed due to shorter scorch safety time. Furthermore, lower S/Ac ratio is very detrimental for rubber-brass adhesion, it should be high for good adhesion.<sup>[28]</sup>

Phase II compounds have been showed desirable rheometric properties, better physicals, and comparable un-aged adhesion. However, the poor extent of adhesion retention suggested for further investigation in resin-based compounds.

### 3.3 | Phase III

In Phase III, aged adhesion was retrieved by adding 5 phr of precipitated silica in phase II compositions. Beside



**FIGURE 5** Showing comparable un-aged adhesion properties and a collapse in adhesion properties after various type of aging treatments for compound [A] and [B] [Color figure can be viewed at wileyonlinelibrary.com]

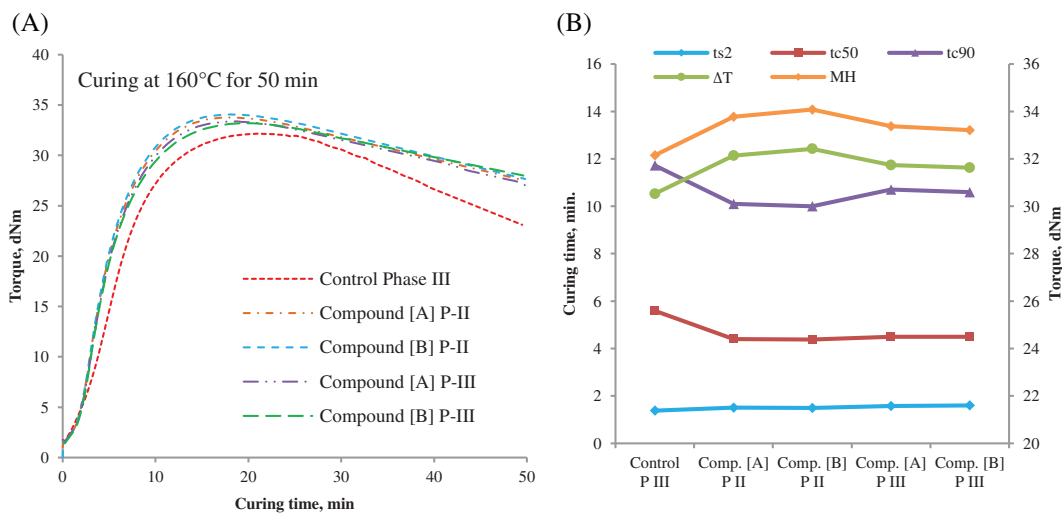
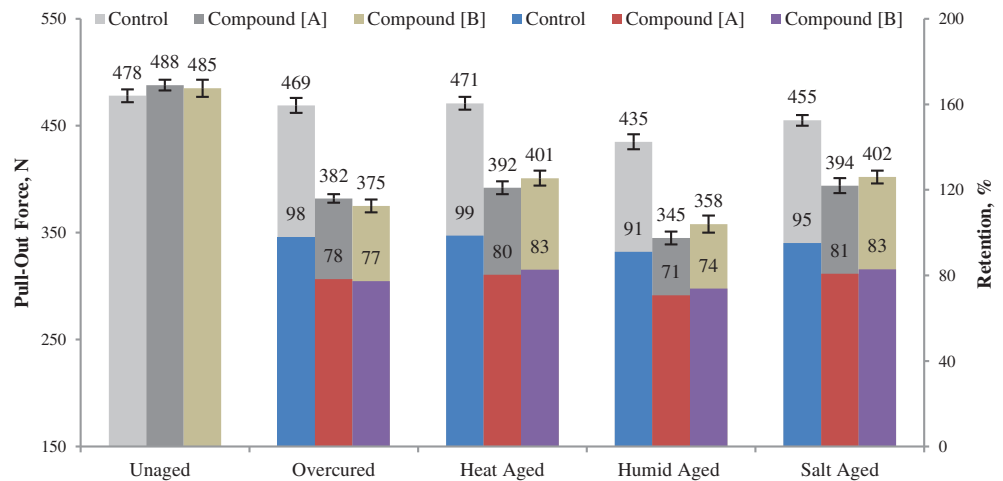


**FIGURE 6** (A) Curing profile at 160°C for 50 min for Phases II and III compounds showing desirable higher stiffness, faster curing, and less reversion than control; (B) showing analysis between various curing parameters from Figure 6 (A) [Color figure can be viewed at wileyonlinelibrary.com]

this, process oil loading was increased from 3 phr to 5 phr, to control the viscosity on silica addition. Due to these modifications, cure properties and physical properties did not change significantly as compared to previous phase. In this phase, since the resin-based compounds were developed as per desired properties that is comparable cure, physical, and adhesion properties, thereby, all three compounds were also examined for the other relevant tests extensively.

### 3.3.1 | Rheometric properties

Figure 6 compares the curing properties obtained in this phase and previous phase. On analyzing Figure 6(B), it has been observed that curing becomes marginally slower

(higher  $t_{c90}$ ) as compared to Phase II, which could be primarily due to the addition of silica. The acidic nature of silica retards cure rate (pH, 6.1).<sup>[22]</sup> The adsorption of the accelerator on the silica surface reduces the cure rate.<sup>[3,29]</sup> Both the resin-based compounds are showing similar cure properties and viscosity. Viscosity values obtained for Control, [A] and [B] are 68, 67, 68, respectively. The addition of silica did not increase the  $M_H$  possibly due to simultaneously enhancement in process oil dose.  $\Delta$ Torque values are found to be similar as compared to previous phase, which is further supported by equal extent of CLD (Figure 4 and Table S3). In previous and this phase, the cure tests were performed for longer time to see the reversion phenomenon. Reversion is the time taken to drop torque up to 98% after attaining maximum level. Figure 6(A) represents less reversion for both

experimental compounds. Reversion time obtained for control, [A] and [B] are 6.01, 6.52, 6.91 min, respectively.

The control compound, containing HMMM and resorcinol, shows a tendency to scorch on storage. In order to study the scorchiness tendency of new resin-based compounds, the MS test was repeated after 14 days of mixing. On analyzing  $t_5$  values from Figure 7 for all three batches, it is evident that control compound has become  $\sim 14\%$  schorchier ( $t_5$  value reduced significantly after 14 days), while compound [A] and [B] showed only 2–3% scorchiness. This fact is presumably due to the no reaction between the resin and HMMM at the ambient storage temperature. Compound [B] showed least scorchiness property. The longer  $t_5$  prevents premature vulcanization during processing and shorter value of cure index ( $\Delta t_L$ ) saves energy during vulcanization.

### 3.3.2 | Physical properties

A graphical representation of physical properties between control compound of Phase III and resin-based compounds of Phases II and III has been shown in Figure S1. In both the phases, resin-based compounds are showing higher stiffness and higher EB, which is desirable for an adhesive compound to perform better under dynamic condition. Steel is a rigid material; therefore, a rigid and stiffer compound is more compatible for better durability.

On analyzing physical properties (Table 7), it is observed that a marginal drop in un-aged modulus of the compound [A] and [B] than the previous phase II. This might be due to the oil dose enhancement. During investigation in this phase, the authors also checked the effect of oxidative (aerobic) and non-oxidative (anaerobic) thermal aging for stress–strain properties, which have been

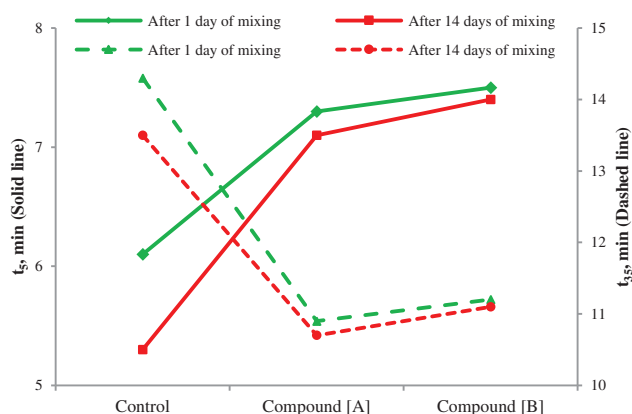


**FIGURE 7** Showing Mooney scorch test results observed in Phase III. Both compounds [A] and [B] are showing very less scorchiness than control on storage [Color figure can be viewed at [wileyonlinelibrary.com](http://wileyonlinelibrary.com)]

shown in the retention form by Figure 8(A),(B). In general, anaerobic aging is given to internal components of a product where environmental oxygen does not reaches. For example, belt skim compound for a tire.

Figure 8(A) shows a percentage drop in properties after anaerobic aging while Figure 8(B) shows a percentage drop and rise in properties after aerobic aging. The percentage change ( $\pm$ ) in physical properties is calculated using Equation (4).

In case of anaerobic aging, a drop in modulus for all compounds is obtained due to decline in CLD undergoes thermal decomposition of crosslinks (softening) via reversion process.<sup>[30]</sup> Compound [A] and [B] have shown less drop in stress–strain properties, which is possibly due to less reversion phenomenon as compared to control. It is also evident from rheographs as presented in Figure 6(A). Compound [B] had shown highest retention in physicals. Figure 8(B) shows that during aerobic aging, compound moduli are increased. This is probably due to CLD enhancement (Table S3) via conversion of poly-sulfidic crosslinks into mono and disulfidic (hardening).<sup>[30]</sup> During both type of aging, TS and EB of all the compounds were dropped via thermal degradation process.<sup>[3]</sup>

Hardness and rebound resilience of phase III compounds are shown in Table S4. Hardness follows the same trend as followed by modulus. It decreased for anaerobic aged samples while increased during aerobic aging. Similar resilience values are observed for compound [A] and [B] at both (ambient and 70°C) temperature but higher than control one. These results indicate low hysteresis nature of the resin-based compounds.

### 3.3.3 | Dynamic mechanical properties

Both resin-based compounds are shown higher elastic modulus ( $E'$ ) and lower  $\tan \delta$  as desirable for a belt skim compound (Figure S2). Greater  $E'$  value indicates higher dynamic stiffness ( $E^*$ ) of the compound, which helps to retain rubber-brass adhesion under dynamic application of the product.<sup>[31]</sup> Lower  $\tan \delta$  value indicates lower hysteresis.<sup>[32]</sup> Compound [B] shows highest  $E'$  and lowest  $\tan \delta$  values at all test temperatures. The higher stiffness of the resin-based compounds is probably caused by higher modulus.

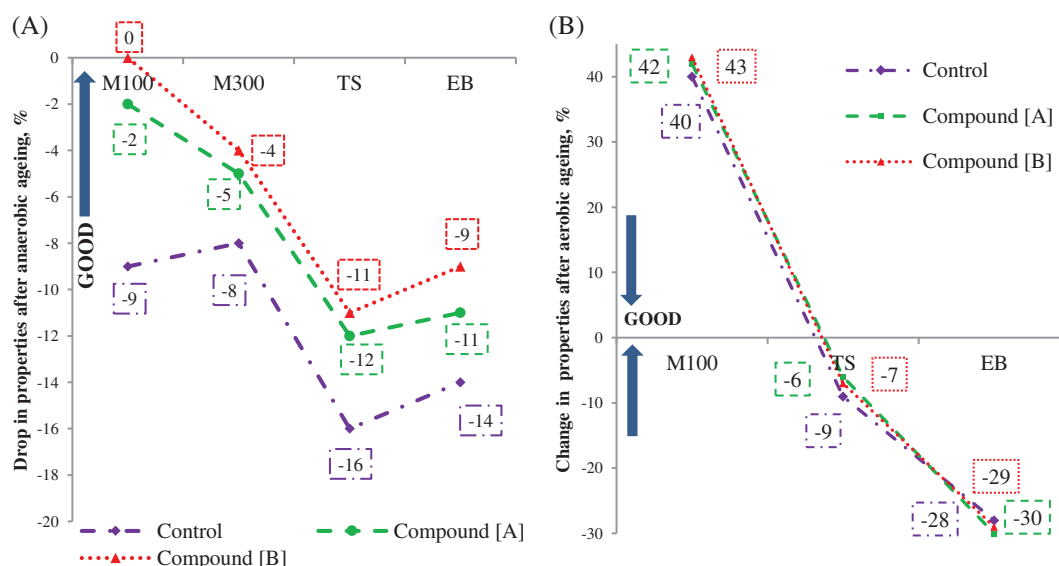
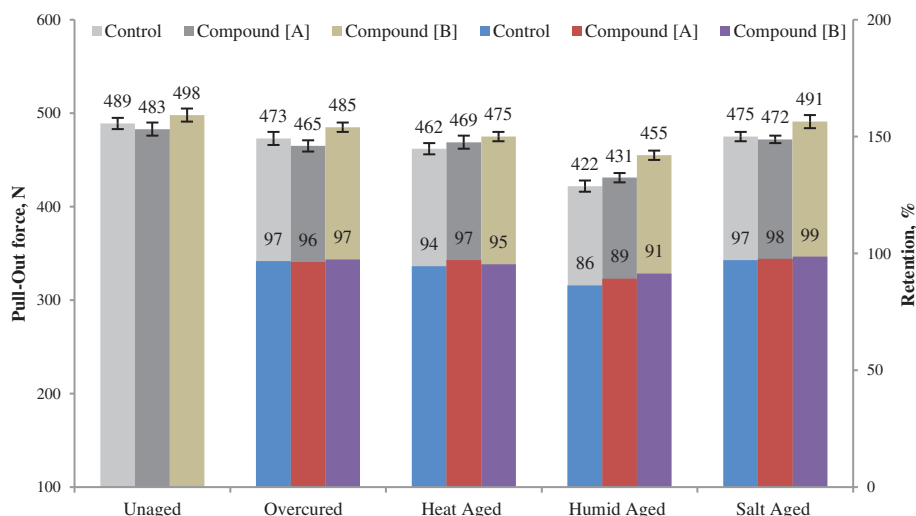
### 3.3.4 | Adhesion properties

The adhesion properties summarized in Figure 9 exhibit that the un-aged adhesion results are almost similar as observed in previous phases. But this time the retention percentage of aged samples is revived for the resin-based

**TABLE 7** Unaged stress strain properties (Phase III)

Test parameter	Control	Compound [A]	Compound [B]
M100 (MPa)	5.5 ( $\pm$ 1)	5.6 ( $\pm$ 1)	5.7 ( $\pm$ 1)
M300 (MPa)	19.6 ( $\pm$ 2)	19.4 ( $\pm$ 1)	19.8 ( $\pm$ 2)
TS (MPa)	21.3 ( $\pm$ 3)	21.8 ( $\pm$ 2)	22.2 ( $\pm$ 3)
EB (%)	350 ( $\pm$ 4)	360 ( $\pm$ 6)	356 ( $\pm$ 5)

Abbreviations: EB, elongation at break; TS, tensile strength.

**FIGURE 8** Analysis of percentage retention in physical properties after aging in Phase III; (A) anaerobic aging: Compound [B] is exhibiting least drop in properties followed by [A] and control; (B) aerobic aging: Both compounds showing comparable retention with respect to control. For heat aging, M300 was not achieved for all three compounds. ([–] and [+] sign on vertical axis in both fig. Indicate a drop and a rise in the physical properties after aging, respectively). The values are nearer to zero, superior the retention [Color figure can be viewed at [wileyonlinelibrary.com](http://wileyonlinelibrary.com)]**FIGURE 9** Showing T-pull adhesion test results obtained from un-aged and differently aged samples [Color figure can be viewed at [wileyonlinelibrary.com](http://wileyonlinelibrary.com)]

compounds, especially in case of compound [B]. This might be associated with the synthesis of protective inter-layer at the adhesion interface by reaction between

HMMM and modified phenolic resins in presence of amorphous precipitated silica. As investigated by D B Russell,<sup>[33]</sup> the addition of silica with adhesion promoting

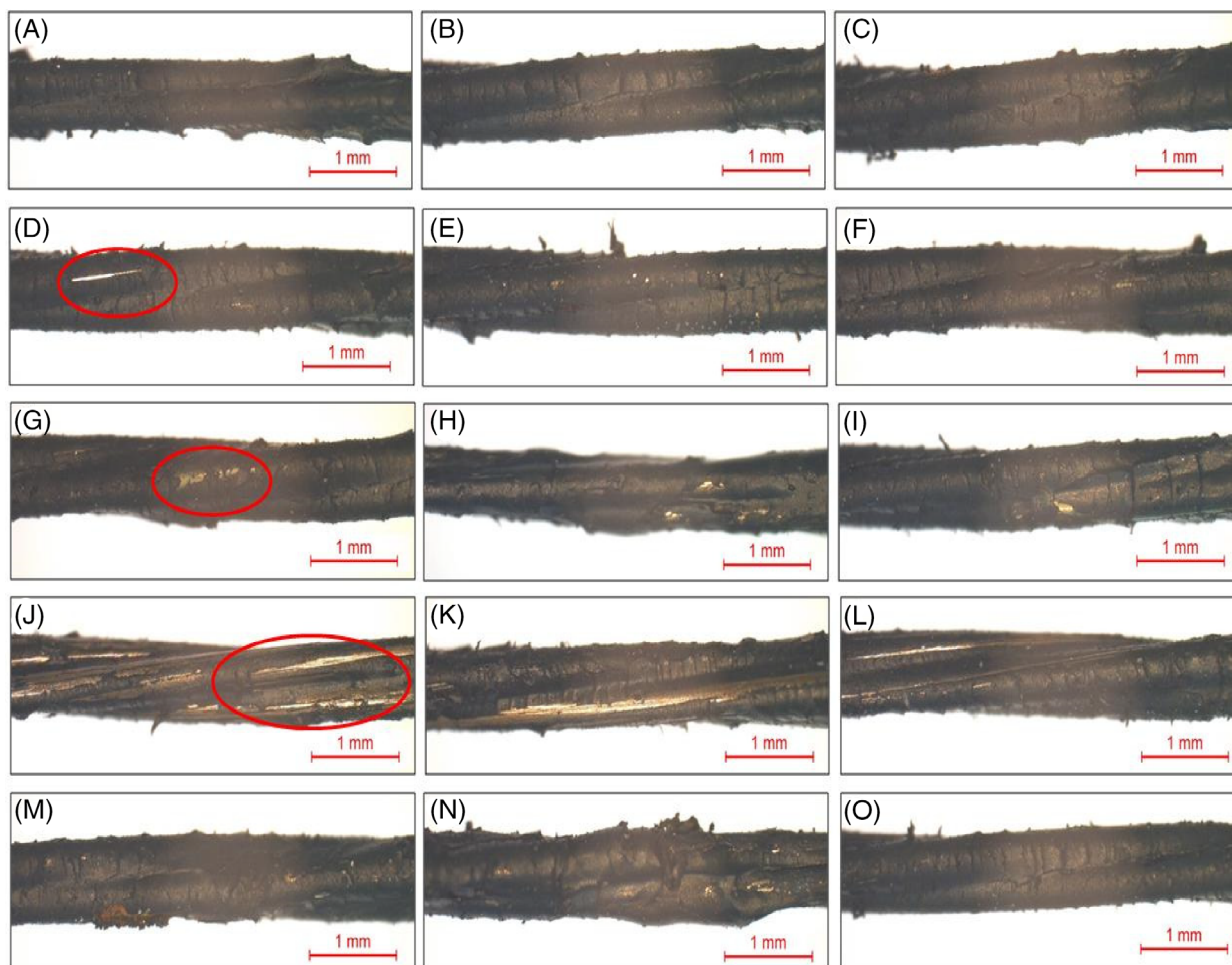


**FIGURE 10** Compound coverage on pulled out cords; (A) U[C], 100% coverage; (B) U[a], 100% coverage; (C) U[B], 100% coverage; (D) O[C], 95% coverage; (E) O[a], 95% coverage; (F) O[B], 100% coverage; (G) T[C], 90% coverage; (H) T[a], 90% coverage; (I) T[B], 95% coverage; (J) H[C], 70% coverage; (K) H[a], 80% coverage; (L) H[B], 90% coverage; (M) S[C], 95% coverage; (N) S[a], 95% coverage; (O) S[B], 100% coverage. U, unaged; O, overcured; T, heat aged; H, humid aged; S, salt aged; C, control [Color figure can be viewed at [wileyonlinelibrary.com](http://wileyonlinelibrary.com)]

system in rubber compounding improves adhesion under severity of aging. The presence of silica retards the extent of reaction between HMMM and phenolic modified resins resulting into formation of low molecular weight fractions of protective complex leads to increased concentration of methylol groups at the interface for the hydrogen bonding.

Furthermore, the presence of silica in combination with cobalt salt, improves the retention of adhesion.<sup>[34]</sup> Similar findings were also perceived by Cochet et al.<sup>[35]</sup> on addition of partial amount of precipitated silica in carbon black filled adhesive compound.

A slight drop in adhesion properties after aging is seen even after, the addition of adhesion promoting system in rubber compounds. This might be due to the compound deterioration during aging, and which is further supported by microscopic images showing cohesive type

failure. After severe aging for longer time, adhesion failure may takes place instead of cohesive failure. Hammer et al. earlier studied and concluded that there is a requirement of an optimal thickness of  $\text{Cu}_x\text{S}$  layer for best adhesion, which prevents the migration of copper ions and also the over thickening of the interlayer.<sup>[36]</sup> The flexible and amorphous  $\text{Cu}_2\text{S}$  form of bonding converts into brittle and crystalline  $\text{CuS}$  form and thus weakens.<sup>[37]</sup> During humidity aging adhesion drops due to the formation of a weak layer of  $\text{ZnO}/\text{Zn}(\text{OH})_2$  and  $\text{Cu}_x\text{S}$  occurs at the metal-rubber interface, which becomes thicker and non-bonding due to bond breakage within this layer.<sup>[8]</sup>

In Phase III, the coverage of cured rubber on steel cord was visually determined for un-aged as well as aged samples and reported along with their microscopic images (magnification: 40 $\times$ ) through Figure 10.

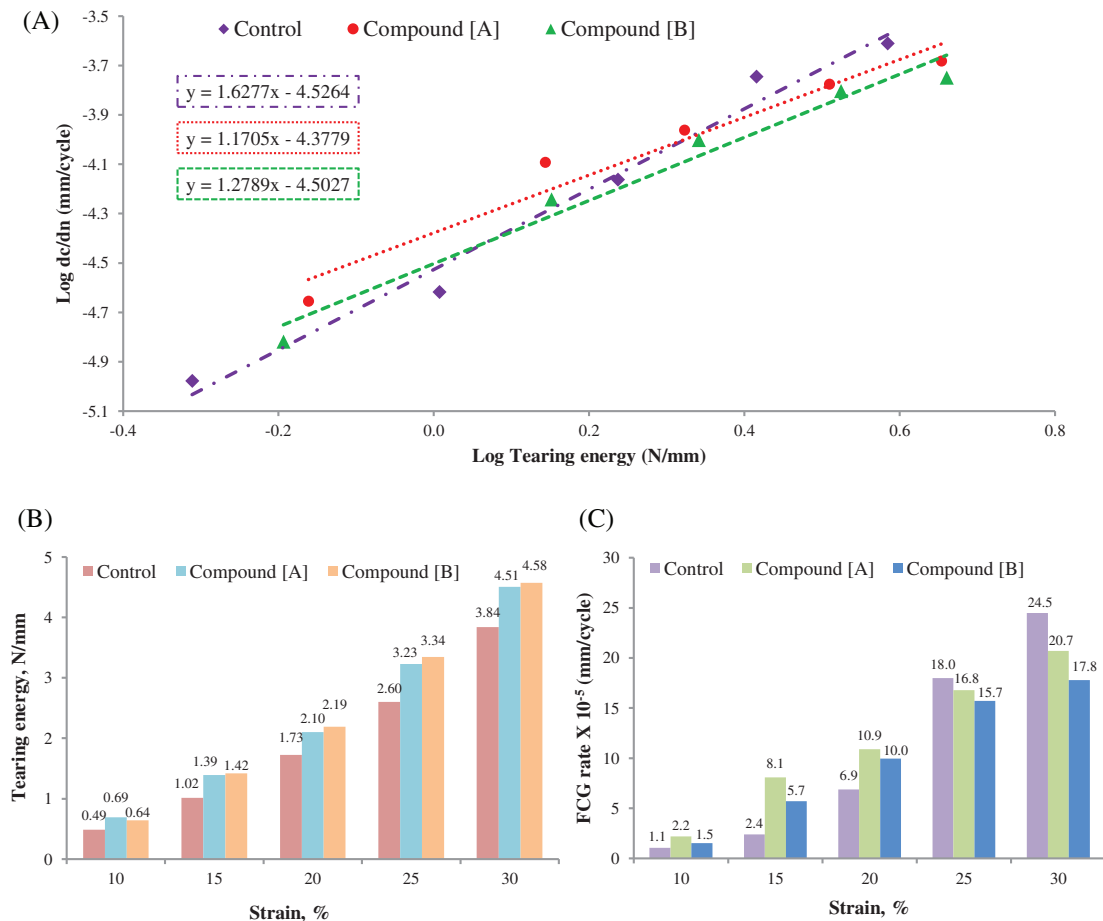


**FIGURE 11** (A) Showing fatigue crack growth rate at various tearing energy for control, compound [A] and [B]; (B) analysis of tearing energy at different strain percentages; (C) analysis of fatigue crack growth rate at different strain percentages [Color figure can be viewed at [wileyonlinelibrary.com](http://wileyonlinelibrary.com)]

### 3.3.5 | Fatigue crack growth

FCG rate of Phase-III compounds has been summarized in Figure 11(A) where a logarithmic plot between  $dc/dn$  and tearing energy (TE) is plotted at different strain percentages. Lower the FCG rate defends better is the durability under dynamic condition. In general, the temperature of PCR tire reaches to around  $70^{\circ}\text{C}$  during service, thus FCG was carried out at the said temperature. It is evident from the Figure 11(A) that as the strain percentage increases both TE and FCG was also increased. A power law dependency is also noticed<sup>[21]</sup> from Figure 11(A), which has been represented mathematically in Equation (8). On analyzing Figure 11(A), it is seen that all three compounds behaved differently in lower and higher TE zone. In low TE zone control compound exhibited least crack growth rate followed by compound [B] and [A] whereas in higher TE zone compound [B] showed least FCG rate followed by compound [A] and control. Among compound [A] and

[B], [A] represented higher FCG rate at all TE and the difference is minimal at higher TE.

From Figure 11(B), it is apparent that TE is increasing with increase in strain percentages. [A] and [B] are showing higher TE as compared to control. The higher modulus and stiffness of the [A] and [B] are the probable reason behind higher TE at all strain percentages. Compound [B] showed highest TE at all strain percentages followed by [A] and control. Figure 11(C) represents the crack growth rate ( $dc/dn$ ) as a function of applied strain for all three compounds. The resin-based compounds have the lower S/Ac ratio (4:1) compared to control (8:1). Therefore, in compound [A] and [B], higher numbers of mono and disulfidic type crosslinks were produced whereas in control compound higher numbers of polysulfidic crosslinks were generated. The polysulfidic linkages are known for higher flexibility and better fatigue life, on the other hand, mono and disulfidic cross linkages exhibit less flexibility and poor fatigue properties.<sup>[21]</sup> So, the less flexibility and higher stiffness of the experimental compounds probably the reason behind higher



FCG rate. Interestingly, after 20% strain, compound [B] exhibited least FCG rate followed by compound [A] and control due to the formation of mono and disulfidic linkage from polysulfidic one at higher strain and temperature.<sup>[38]</sup>

## 4 | CONCLUSIONS

Sustainable development required focus on removal of all carcinogenic and hazardous substance from the product during manufacturing and also in service condition. This study aims to support this novel movement by developing rubber compounds without any hazardous material. In this research, belt-skim compound has been developed with two kinds of experimental resins [A] and [B] by the replacement of resorcinol to have superior contribution in adhesion mechanism. These resins neither generate fumes nor any hazardous substance during processing at high temperature whereas resorcinol emits carcinogenic fumes at the same condition. This study conducted in three phases with the replacement of 1:1 ratio to regulate all the properties. Both compounds with resin [A] and [B] have shown improved physical, dynamic mechanical, and adhesion properties in un-aged as well as aged conditions in comparison to the control one. Although [A] and [B] exhibited a little bit higher crack growth rate at up to 20% strain but overall properties of compound [B] was found to be better than [A]. Therefore, this study finds a way forward to eliminate hazardous material from the tire compound to develop sustainable technology for green mobility.

## ACKNOWLEDGMENTS

The authors are very thankful to the Hari Shankar Singhanian Elastomer and Tire Research Institute (HASETRI) for their kind support and permission in publishing this research work.

We also extended our acknowledgment to Mr. Ramesh Shilavant and Mr. Nitish Mishra for their contribution toward microscopic analysis and FCG characterization on our behalf.

## ORCID

Jagannath Chanda  <https://orcid.org/0000-0002-9671-028X>

## REFERENCES

- [1] W. J. Van Ooij, P. B. Harakuni, G. Buytaert, *Rubber Chem. Technol.* **2009**, 82, 315.
- [2] P. Y. Patil, W. J. Van Ooij, *Rubber Chem. Technol.* **2004**, 77, 891.
- [3] G. S. Jeon, *J. Adhes. Sci. Technol.* **2008**, 22, 1223.
- [4] R. B. Durairaj, *Resorcinol: Chemistry, Technology and Applications*, Vol. I, Springer, Berlin, Germany **2005**, p. 228.
- [5] W. S. Fulton, *Rubber Chem. Technol.* **2005**, 78, 426.
- [6] G. Haemers, J. Mollet, *J. Elastomers Plast.* **1978**, 10, 241.
- [7] T. Hotaka, Y. Ishikawa, *Rubber Chem. Technol.* **2005**, 78, 175.
- [8] W. J. Van Ooij, *Rubber Chem. Technol.* **1984**, 57, 421.
- [9] J. F. Beecher, *Surf. Interfaces Anal.* **1991**, 17, 245.
- [10] P. Persoone, R. De Gryse, P. De Volder, *J. Electron Spectrosc. Relat. Phenomenon* **1995**, 71, 225.
- [11] G. S. Jeon, J. Adhes, *J. Sci. Technol.* **2003**, 17, 797.
- [12] G. Haemers, *Rubber World* **1980**, 182, 26.
- [13] A. K. Chandra, A. Biswas, R. Mukhopadhyay, A. K. Bhowmik, *J. Adhes.* **1994**, 44, 177.
- [14] A. K. Chandra, A. S. Deuri, R. Mukhopadhyay, A. K. Bhowmik, *Kautsch. Gummi Kunstst.* **1997**, 50, 106.
- [15] J. M. Dreyfors, S. B. Jones, Y. Sayed, *Am. Ind. Hygiene Assoc. J.* **1989**, 50, 579.
- [16] A. K. Chandra, A. Biswas, R. Mukhopadhyay, et al., *J. Adhes. Sci. Technol.* **1996**, 10, 431.
- [17] G. R. Hamed, J. Huang, *Rubber Chem. Technol.* **1991**, 64, 285.
- [18] S. G. Choudhry, J. Chanda, S. Ghosh, K. Banerjee, S. S. Banerjee, A. Das, P. Ghosh, S. K. Bhattacharyya, R. Mukhopadhyay, *Polym. Eng. Sci.* **2020**, 60, 1973.
- [19] M. Liu, B. J. Rohde, R. Krishnamoorti, M. L. Robertson, M. Dawood, *Polym. Eng. Sci.* **2020**, 60, 104.
- [20] S. Dasgupta, S. L. Agrawal, S. Bandyopadhyay, S. Chakraborty, R. Mukhopadhyay, R. K. Malkani, S. C. Ameta, *Polym. Test.* **2008**, 27, 277.
- [21] P. Ghosh, R. Stocck, M. Gehde, R. Mukhopadhyay, R. Krishnakumar, *Int. J. Fracture* **2014**, 188, 9.
- [22] H. Sridharan, A. Guha, S. Bhattacharyya, A. K. Bhowmik, R. Mukhopadhyay, *Rubber Chem. Technol.* **2019**, 92, 326.
- [23] G. Andreini, P. Straffi, S. Cotugno, G. Gallone, G. Polacco, *Rubber Chem. Technol.* **2013**, 86, 132.
- [24] H. Sridharan, J. Chanda, P. Ghosh, R. Mukhopadhyay, *Prog. Rubber Plast. Recycling Technol.* **2020**, 36, 115.
- [25] R. B. Durairaj, *Resorcinol: Chemistry, Technology and Applications*, Vol. I, Springer, Berlin, Germany **2005**, p. 245.
- [26] Y. Chokanandsombat, C. Sirisinha, *Polym. and Polym. Compos.* **2014**, 22(7), 599.
- [27] M. J. Wang, *Rubber Chem. Technol.* **1998**, 71, 520.
- [28] G. R. Hamed, T. Donatelli, *Rubber Chem. Technol.* **1983**, 56, 450.
- [29] F. Yatsuyanagi, N. Suzuki, M. Ito, H. Kaidou, *Polym. J.* **2002**, 34, 332.
- [30] R. Mukhopadhyay, *Introduction of Polymer Science & Rubber Technology*, Vol. 1, Indian Rubber Institute, Rajasthan, India **2002**, p. 163.
- [31] A. N. Gent, G. S. Fielding-Russell, D. I. Livingston, D. W. Nicholson, *J. Mater. Sci.* **1981**, 16, 949.
- [32] S. L. Agrawal, S. Bandyopadhyay, S. Dasgupta, R. Mukhopadhyay, *Rubber World* **2008**, 237(4), 31.
- [33] J. Creasey, D. Russell, M. Wagner, *Rubber Chem. Technol.* **1968**, 41, 1300.
- [34] W. H. Wadell, *Rubber World* **1997**, 216, 22.
- [35] P. Cochet, D. Butcher, Y. Bomal, *Kautsch. Gummi Kunstst.* **1995**, 48, 353.
- [36] G. E. Hammer, R. M. Shemanski, J. D. Hunt, *J. Vacuum Sci. Technol. A.* **1994**, 12, 2388.



[37] P. Y. Patil, W. J. Van Ooij, *Rubber Chem. Technol.* **2006**, 79, 82.

[38] S. G. Kim, S. H. Lee, *Rubber Chem. Technol.* **1994**, 67, 649.

### SUPPORTING INFORMATION

Additional supporting information may be found online in the Supporting Information section at the end of this article.

**How to cite this article:** Kumawat P, Chanda J, Das SK, Ghosal A, Gupta SD, Mukhopadhyay R. Alternatives of resorcinol in carbon black filled belt skim compound: A sustainable approach to make tire. *Polym Eng Sci.* 2021;1–15. <https://doi.org/10.1002/pen.25635>